Automatic Extraction of Building Footprints from LIDAR Using Image Based Methods

ZhenYang Hui*, YouJian Hu, and Peng Xu

Faculty of Information Engineering, China University of Geosciences, Wuhan 430074, P.R. China
huizhenyang2008@163.com

Abstract. This paper proposes a method by which scattered LIDAR point clouds are converted into a two-dimensional image and then building footprints are extracted through the image processing. Firstly point cloud grid is handled to generate georeferenced feature image, and then image threshold segmentation, morphological close operation, connectivity analysis and contour tracking method is used to obtain the final building footprints. Finally, based on the mapping relationship between georeferenced feature image and scattered point clouds, building outline points are obtained. Experimental result shows that this method could extract building footprints very well in plain area, but due to the adoption of single image segmentation method in the georeferenced feature image, it is not suitable for the building footprints extraction in mountainous area.

Keywords: LIDAR georeferenced feature image, image threshold segmentation, morphological close operation, connectivity analysis, automatic building footprints extraction.

1 Introduction

Airborne laser scanner (ALS) is a new technical measure which is developing very rapidly in recent years. Due to its ability to quickly obtain space 3d information, nowadays it is widely used in 3d city modeling and spatial information analysis [1]. In the 3d city modeling, building is the main entity of spatial information. Therefore, it is of great research value to extract the building footprints information from LIDAR point clouds quickly and accurately. Fig. 1 shows the measurement process of airborne LIDAR system [2].

Methods of building footprints extraction have been extensively studied at home and abroad in recent years. Haithcoat, et al. (2001) set different thresholds to extract building footprints from LIDAR point clouds by adopting different height and shape characteristics [3]. Zhang, et al. (2006) used region growing and plane fitting methods to distinguish building from vegetation with the help of normalized DSM (nDSM) [4]. Li, et al. (2008) firstly eliminated lower ground objects through setting threshold, and

* Corresponding author.

F. Bian and Y. Xie (Eds.): GRMSE 2014, CCIS 482, pp. 79–86, 2015.

then used morphological open operation to interrupt the non-building part attached to the building. Finally, he used region growing method to detect the connection area and then clustered buildings [5]. Al-Durgham, et al. (2012) firstly used region growing method to extract plane, and then adopted the improved convex hull algorithm to estimate rough outline of the roof. Finally, he used recursive minimum bounding rectangle method and Boolean operator to produce the final rules and boundaries [6].

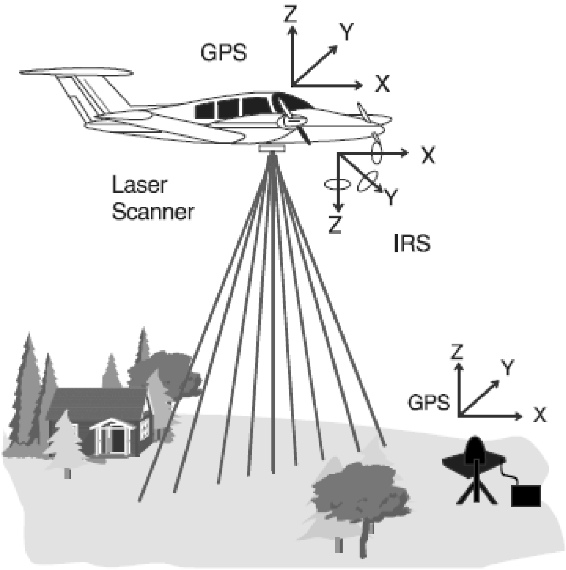

Fig. 1. Sketch map of LIDAR scanning (Flood and Gutelius, 1997)

All methods above can extract building footprints with good effects, but most of them are more complicated. Due to the huge number of LIDAR point clouds, complicated methods always need more complex computer computation and longer computing time, which is against the will of quick spatial information acquired by using airborne radar. Therefore, it is very necessary to design a simple, rapid and effective building footprints extraction method.

2 Building Footprints Extraction

Airborne LIDAR point clouds mainly contain three-dimensional coordinate information, so we cannot conduct point clouds classification and feature extraction directly. The main train of thought of the method proposed by this paper is that elevation values can be converted to grayscale values through grid handling, which can be generated georeferenced feature image. And then through image threshold segmentation, morphological close operation, connectivity analysis and contour tracking, building footprints can be extracted. Fig. 2 elaborates the processing flow chart.

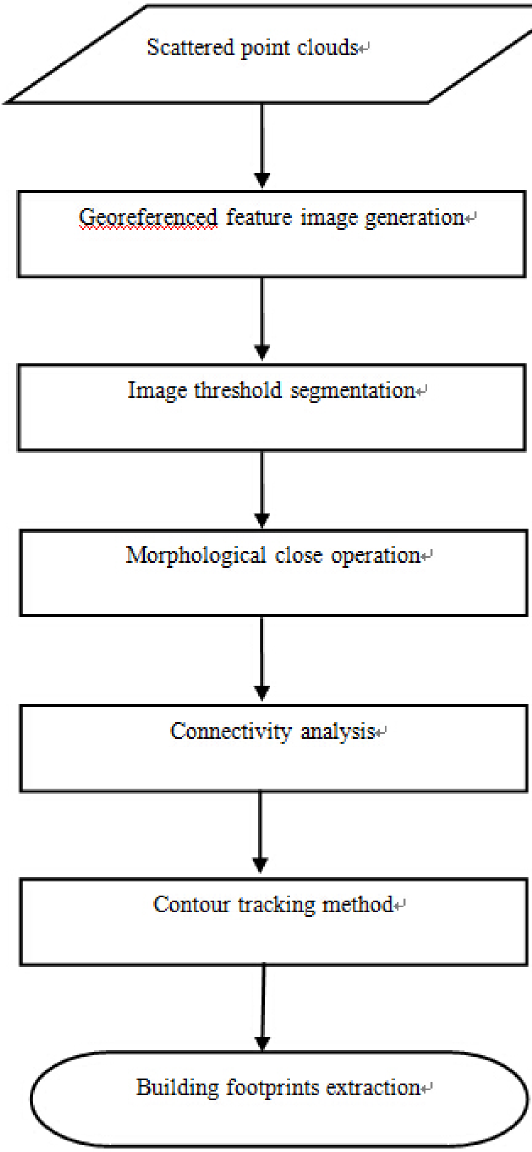

Fig. 2. The flow chart of the proposed method

2.1 Georeferenced Feature Image Generation

To turn scattered point clouds into two-dimensional image, firstly what needs to do is grid handling which can project the scanned points onto X-Y plane. Then according to certain rules elevation values can be converted to gray values. Finally, characteristic value of each cell should be calculated to generate a georeferenced feature image.

(1) Point clouds grid handling

First of all, cell size (dH) should be determined on the basis of point clouds sampling interval. The minimum and maximum values of X, Y ($X_{\min}$, $Y_{\min}$, $X_{\max}$, $Y_{\max}$) can be obtained from the three-dimensional coordinate information of point clouds. And then width (W) and height (H) of the georeferenced feature image and grid number of individual point $(X_{num}(i), Y_{num}(i))$ can be calculated as below.

$$\begin{cases} W = floor((X_{\max} - X_{\min})/dH) + 1 \\ H = floor((Y_{\max} - Y_{\min})/dH) + 1 \end{cases} . \tag{1}$$

$$\begin{cases} X_{num}(i) = floor((X(i) - X_{\min})/dH) + 1 \\ Y_{num}(i) = floor((Y(i) - Y_{\min})/dH) + 1 \end{cases} . \tag{2}$$

(2) Characteristic value of each cell calculation

The minimum and maximum of Z coordinates ($Z_{\min}$, $Z_{\max}$) can be obtained from point clouds data. According to the following equation elevation values can be converted to gray values.

$$Z_{gray}(i) = \frac{Z(i) - Z_{\min}}{Z_{\max} - Z_{\min}} \times 255 . \tag{3}$$

Then we can use Eq. (4) to calculate the average gray value of each cell which can be regarded as the characteristic value of each cell. If the number of point clouds within the cell is 0, characteristic value of this cell should be assigned 0, performing black on the 2d image. After finishing this, the georeferenced feature image is generated.

$$Z_{num\_gray}(i) = \sum_{j=1}^{n} Z_{gray}^{j}(i) \Big/ n . \tag{4}$$

2.2 Image Threshold Segmentation

In light of buildings, trees and other landforms onto the generated georeferenced feature image all have different gray values, this paper adopts OTSU algorithm to do image segmentation.

Firstly, we can initialize a gray value k . With this, georeferenced feature image can be divided into two types of target and background. Then we should calculate the probability (ω_1 , ω_2) and average (μ_1 , μ_2) of the two kinds. After this, the variance ($\sigma^2(k)$) between the two kinds of classes can be calculated.

$$\sigma^2(k) = \omega_1(\mu_1 - \mu)^2 + \omega_2(\mu_2 - \mu)^2 . \tag{5}$$

Where μ is the mean gray value of georeferenced feature image.

Through constantly iterative calculation, once $\sigma^2(k)$ reaches maximum, at this time the gray value k is requested. The targets whose gray values are greater than k are buildings[7].

2.3 Morphological Close Operation

After image threshold segmentation the georeferenced feature image is performed as binary image, in which buildings are white color. In order to eliminate small hole on the binary image and repair the broken contour line to make it more smooth, we need to do morphological close operation.

Morphological close operation can be defined according to the following formula. That is to say the structural element B to set A morphological close operation is to use B to do first expansion for A, and then use B to do second corrosion for the result.

$$A \bullet B = (A \oplus B)\Theta B \quad . \tag{6}$$

Among them, corrosion is to lead the outline to internal contraction, which can help eliminate the outline points. While expansion is to contact with the object of all the background to the object, which can make the outline expand to external [8].

2.4 Connectivity Analysis

Due to the influence of external environment, point clouds data obtained by airborne radar always has gaps, which would cause a same roof of the house to be broken into two or more pieces embodied in the two-dimensional image. To solve this problem, we should do connectivity analysis. Connected in image processing usually refers to four connected or eight connected, which one to chose can be decided according to actual processing effect.

Another function of connectivity analysis is to do the second judge for the target building. After the image threshold segmentation, some high trees, utility poles and high tension lines also would be mistaken for the target building. To avoid this situation, we should set an area threshold to judge the connected area of binary image, the one whose area is less than it should be weeded out.

2.5 Contour Tracing Method

To extract building footprints from connected binary image, a contour tracing method proposed by Pavlidis (1982) can be applied [9]. After finding building footprints in binary image, we can extract building outline points from LIDAR points according to the mapping relationship between image and point clouds data.

3 Experiment and Analysis

The experimental data comes from eight scenes data located in Vaihingen/Enz test field and the center of Stuttgart city which was obtained by ISPRS Commission

Ⅲ Working Group Ⅲ/3 (http://www.itc.nl/isprswgIII-3/filtertest/index.html). To test the effectiveness of the algorithm proposed by this paper, the experiment uses S31 datasets as representative, which contains high density cement roof constructions, ups and downs vegetations and data gaps. The total number of S31 sample point clouds data is 28862. The point spacing is 1-1.5m and point density is 0.67 per square meter [8].

3.1 Georeferenced Feature Image Generation

To make sure that most cells contain at least one point and the georeferenced feature image is without distortion, the cell size here is set to be 2m. After characteristic value of each cell calculation, we can get the final georeferenced feature image. As shown in Fig. 3, cells without point were turned out to be black, while roads and some low plants were characterized by dark color as their gray values were small. The roof of the building as well as some tall trees whose gray values were lager was characterized by bright color. Hence, the georeferenced feature image preserved the original shape information of the building very well.

3.2 Image Threshold Segmentation Outcome

As shown in Fig. 4, after image threshold segmentation the georeferenced feature image performed as binary image. The shape of buildings can be clearly recognized from the image. The reason why the borders are jagged is mainly result of grid handling, which has no effect on the extraction of building footprints. Some small white patches are caused by high trees or poles.

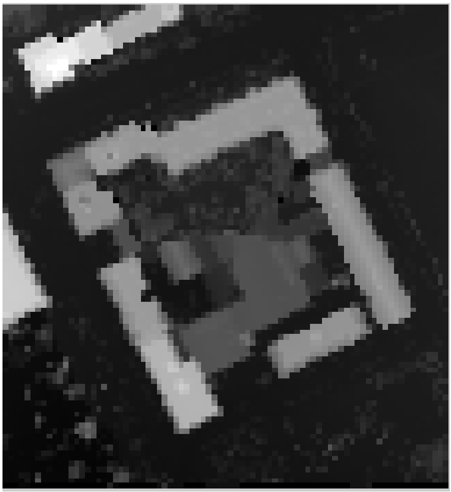

Fig. 3. Georeferenced feature image

Fig. 4. Binary image

3.3 Connectivity Analysis Outcome

Here we adopted four connected processing method and set the area threshold to be 20 m^2. In order to facilitate subsequent contour tracking, the transform was made for the binary image to turn the building to be black color. As shown in Fig. 5, after connectivity analysis the two houses at the lower right corner were connected together, which was in line with the field situation. In addition, some small patches whose areas were less than threshold were also removed.

3.4 Building Footprints Extraction Outcome

Applied the contour tracing algorithm to the binary image, we can get the final building outline, as shown in Fig. 6. Then according to the mapping relationship between georeferenced feature image and point clouds data, we can get 3d coordinates of building outlines.

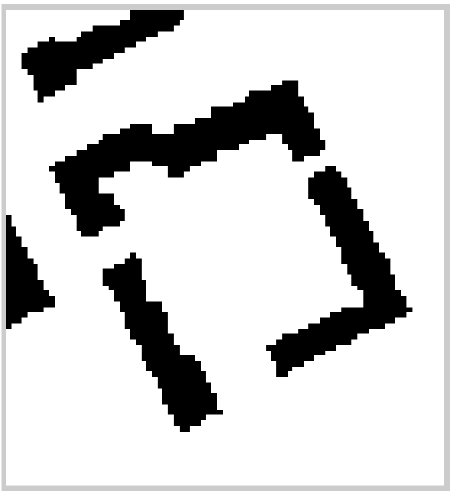

Fig. 5. Building shape after connectivity analysis

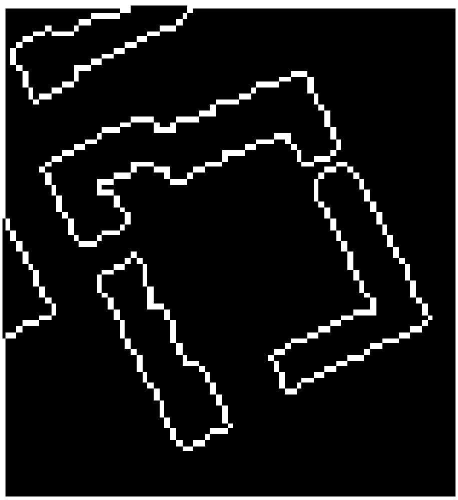

Fig. 6. Final building outlines

4 Conclusion

The method proposed by this paper firstly converts LIDAR point clouds to image information and then do a series of operation to the 2d image. The principle of this method is simple and it needs a small amount of calculation. From the experimental analysis, we can get that this method can extract the building footprints effectively and it can apply to most of plain area for building footprints extraction. As this method adopts single threshold segmentation method, it is prone to miscarriage in the mountainous area [10]. This also is what needs to be improved for this method.

Acknowledgments. The experimental datasets were provided by ISPRS Commission Ⅲ Working Group Ⅲ/3. Thanks very much for their hard work. In addition, the authors would like to thank anonymous reviewers for their insightful suggestions and comments.

References

1. Flood, M., Gutelius, B.: Commercial Implication of Topographic Terrain Mapping Using Scanning Airborne Laser Radar. Photogrammetric Engineering and Remote Sensing 63(4), 327–366 (1997)
2. Vosselman, M.G., Kessels, P., Gorte, B.G.H.: The Utilization of Airborne Laser Scanning for Mapping. International Journal of Applied Earth Observation and Geoinformation 6(3/4), 177–186 (2005)
3. Haithcoat, T.L., Song, W., Hipple, J.D.: Building Footprint Extraction and 3-D Reconstruction from LIDAR Data. In: Proceedings of the Remote Sensing and Data Fusion over Urban Areas, pp. 74–78. IEEE/ISPRS, Roma (2001)
4. Zhang, K., Yan, J., Chen, S.C.: Automatic Construction of Building Footprints from Airborne Lidar Data. IEEE Transactions on Geoscience and Remote Sensing 44(9), 2523–2533 (2006)
5. Li, Y., Wu, H.Y.: Automatic Building Detection Using LIDAR Data and Multispectral Imagery. International Archives of the Photogrammetry, Remote Sensing and Spatial Information Sciences 37(pt. B1), 197–202 (2008)
6. Al-Durgham, M., Kwak, E., Habib, A.: Automatic Extraction of Building Outlines from LiDAR Using the Minimum Bounding Rectangle Algorithm. In: Global Geospatial Conference (2012)
7. Otsu, N.: A Threshold Selection Method from Gray-Level Histogram. IEEE Transactions on Systems Man Cybernetics 9(1), 62–66 (1979)
8. Chen, Q., Gong, P., Baldocchi, D.D., et al.: Filtering Airborne Laser Scanning Data with Morphological Methods. Photogrammetric Engineering and Remote Sensing. 73(2), 175–185 (2007)
9. Pavlidis, T.: Algorithms for Graphics and Image Processing. Computer Science Press. Rockville (1882)
10. Hui, Z.Y., Wu, B.P., Xu, P., Guo, J.X.: Three-dimensional Laser Scanning Topographic Data Acquisition Processing. Science Technology and Engineering 14(18), 1–3 (2014)